

# SIMULTANEOUS MULTI-WAVELENGTH OBSERVATIONS OF MAGNETIC ACTIVITY IN ULTRACOOL DWARFS. I. THE COMPLEX BEHAVIOR OF THE M8.5 DWARF TVLM 513-46546

E. BERGER<sup>1,2,3</sup>, J. E. GIZIS<sup>4</sup>, M. S. GIAMPAPA<sup>5</sup>, R. E. RUTLEDGE<sup>6</sup>, J. LIEBERT<sup>7</sup>, E. MARTÍN<sup>8,9</sup>,  
G. BASRI<sup>10</sup>, T. A. FLEMING<sup>7</sup>, C. M. JOHNS-KRULL<sup>11</sup>, N. PHAN-BAO<sup>9</sup>, W. H. SHERRY<sup>5</sup>

*Draft version October 25, 2018*

## ABSTRACT

We present the first simultaneous radio, X-ray, ultraviolet, and optical spectroscopic observations of the M8.5 dwarf TVLM 513-46546, with a duration of 9 hours. These observations are part of a program to study the origin of magnetic activity in ultracool dwarfs, and its impact on chromospheric and coronal emission. Here we detect steady quiescent radio emission superposed with multiple short-duration, highly polarized flares; there is no evidence for periodic bursts previously reported for this object, indicating their transient nature. We also detect soft X-ray emission, with  $L_X/L_{\text{bol}} \approx 10^{-4.9}$ , the faintest to date for any object later than M5, and a possible weak X-ray flare. TVLM 513-46546 continues the trend of severe violation of the radio/X-ray correlation in ultracool dwarfs, by nearly 4 orders of magnitude. From the optical spectroscopy we find that the Balmer line luminosity exceeds the X-ray luminosity by a factor of a few, suggesting that, unlike in early M dwarfs, chromospheric heating may not be due to coronal X-ray emission. More importantly, we detect sinusoidal H $\alpha$  and H $\beta$  equivalent width light curves with a period of 2 hr, matching the rotation period of TVLM 513-46546. This is the first known example of such Balmer line behavior, which points to a co-rotating chromospheric hot spot or an extended magnetic structure, with a covering fraction of about 50%. This feature may be transitory based on the apparent decline in light curve peak during the four observed maxima. From the radio data we infer a large scale and steady magnetic field of  $\sim 10^2$  G, in good agreement with the value required for confinement of the X-ray emitting plasma. A large scale field is also required by the sinusoidal Balmer line emission. The radio flares, on the other hand, are produced in a component of the field with a strength of  $\sim 3$  kG and a likely multi-polar configuration. The overall lack of correlation between the various activity indicators suggests that the short duration radio flares do not have a strong influence on the chromosphere and corona, and that the chromospheric emission may not be the result of coronal heating.

*Subject headings:* radio continuum:stars — stars:activity — stars:low-mass, brown dwarfs — stars:magnetic fields

## 1. INTRODUCTION

In recent years it has become evident that low mass stars and brown dwarfs (spectral classes late-M and L) are capable of producing unanticipated levels of magnetic activity, manifested primarily in their strong quiescent and flaring radio emission (Berger et al. 2001; Berger 2002; Berger et al. 2005; Burgasser & Putman 2005; Berger 2006; Osten et al. 2006b; Antonova et al. 2007; Phan-Bao et al. 2007; Hallinan et al. 2007; Audard et al. 2007). Other traditional activity indicators such as chromospheric Balmer line emission and coronal X-ray emission, however, appear to steeply decline from peak levels in early and mid M

dwarfs (Pallavicini et al. 1981; Vilhu & Walter 1987; Gizis et al. 2000; West et al. 2004), leading to divergent trends of magnetic activity at the bottom of the main sequence. In both H $\alpha$  and X-rays there is also a clear transition from persistent emission to a small number of flaring objects with duty cycles of a few percent (Reid et al. 1999; Gizis et al. 2000; Rutledge et al. 2000; Liebert et al. 2003; West et al. 2004), as well as a breakdown of the rotation-activity relation (Basri & Marcy 1995; Mohanty & Basri 2003) that is clearly seen in early M dwarfs (Rosner et al. 1985; Fleming et al. 1993; Mohanty et al. 2002; Pizzolato et al. 2003).

The change and divergence in activity trends is most

<sup>1</sup>Observatories of the Carnegie Institution of Washington, 813 Santa Barbara Street, Pasadena, CA 91101

<sup>2</sup>Princeton University Observatory, Peyton Hall, Ivy Lane, Princeton, NJ 08544

<sup>3</sup>Hubble Fellow

<sup>4</sup>Department of Physics and Astronomy, University of Delaware, Newark, DE 19716

<sup>5</sup>National Solar Observatory, National Optical Astronomy Observatories, Tucson, AZ 85726

<sup>6</sup>Department of Physics, McGill University, Rutherford Physics Building, 3600 University Street, Montreal, QC H3A 2T8, Canada

<sup>7</sup>Department of Astronomy and Steward Observatory, University of Arizona, 933 North Cherry Avenue, Tucson, AZ 85721

<sup>8</sup>Instituto de Astrofísica de Canarias, C/ Vía Láctea s/n, E-38200 La Laguna, Tenerife, Spain

<sup>9</sup>University of Central Florida, Department of Physics, PO Box 162385, Orlando, FL 32816

<sup>10</sup>Astronomy Department, University of California, Berkeley, CA 94720

<sup>11</sup>Department of Physics and Astronomy, Rice University, 6100 Main Street, MS-61 Houston, TX 77005

clearly evident in the breakdown of the radio/X-ray correlation that holds for a large number of early-type stars and solar flares (Guedel & Benz 1993; Gudel et al. 1993a; Benz & Guedel 1994), and is attributed to flare heating of coronal plasma to X-ray temperatures (Neupert 1968; Guedel et al. 1996). While objects in the range M0–M6 obey this correlation, several objects later than M7 exhibit radio emission that is several orders of magnitude brighter than expected (Berger et al. 2001; Berger 2002; Berger et al. 2005; Berger 2006). Similarly, in early M dwarfs there is an overall energy balance between X-ray and chromospheric emission, which has led to the idea of chromospheric heating by coronal X-rays (e.g., Cram 1982; Hawley et al. 1995). It is not known whether this mechanism holds in ultracool dwarfs, primarily because of the decline in persistent activity.

Theoretical work on magnetic dynamos in ultracool dwarfs also remains inconclusive. Studies of the  $\alpha^2$  dynamo in fully convective stars suggest that a stratified and rotating turbulent medium can lead to the build-up of a non-axisymmetric and multi-polar field (e.g., Chabrier & Küker 2006; Dobler et al. 2006), but these models make several simplifications for computational purposes. It has also been argued that decreasing electrical conductivity will impede the dissipation of any magnetic fields in the cool and increasingly neutral atmospheres of ultracool dwarfs (Mohanty et al. 2002). The existing radio detections suggest that field dissipation may not be a problem, but the overall field configuration and the effect of neutral atmospheres in the presence of magnetic dissipation remain largely unexplored.

As a result of the various conflicting trends and the transition from persistent to flaring emission, progress in our understanding of magnetic activity and dynamos in ultracool dwarfs requires *simultaneous* observations of the various activity bands. We have already undertaken such observations for the L3.5 brown dwarf 2MASS J00361617+1821104 in late 2002 and discovered periodic radio emission ( $P = 184$  min), with no corresponding X-ray or H $\alpha$  emission (Berger et al. 2005). These observations indicated a magnetic field of  $\sim 200$  G covering a substantial fraction of the stellar surface, as well as the first direct confirmation that the radio/X-ray correlation is indeed violated by orders of magnitude. Follow-up observations showed that the field is stable on a  $\gtrsim 3$  yr timescale, much longer than the convective turnover time, pointing to a stable dynamo process. A recent simultaneous observation of the L dwarf binary Kelu-1 resulted in an X-ray detection without corresponding radio emission (Audard et al. 2007), although the radio limits still allow for a violation of the radio/X-ray correlation by up to  $\sim 2 \times 10^3$ .

Here we exploit the powerful approach of simultaneous observations to investigate the magnetic activity in the M8.5 dwarf TVLM 513-46546, an object previously detected in the radio (Berger 2002, 2006; Osten et al. 2006b; Hallinan et al. 2006, 2007) and in H $\alpha$  (Martin et al. 1994; Reid et al. 2002; Mohanty & Basri 2003). These observations are the first in a series that targets several objects in the sparsely-studied and critical spectral type range M7 to

L3. In the case of TVLM 513-46546 we detect radio, X-ray, and Balmer line emission, but no UV emission. The overall behavior is complex and largely uncorrelated between the various emission bands. The long time and wavelength baselines provide unprecedented detail, including the first case to date of sinusoidal Balmer line emission; the observed 2-hour period is in excellent agreement with the rotation of TVLM 513-46546. Using the various activity indicators we infer the properties of the magnetic field, corona, and chromosphere, and show that the underlying processes and field configuration likely differ from those in early M dwarfs.

## 2. OBSERVATIONS

We targeted the M8.5 dwarf TVLM 513-46546 due to its vicinity ( $d = 10.6$  pc; Dahn et al. 2002) and known radio and H $\alpha$  activity. The bolometric luminosity of TVLM 513-46546 is  $L_{\text{bol}} \approx 10^{-3.59} L_{\odot}$ , and its rotation velocity is  $v \sin i \approx 60$  km s $^{-1}$  (Mohanty & Basri 2003). The non-detection of lithium, with a limit of 0.05 Å, suggests that TVLM 513-46546 is most likely a very low mass star (Reid et al. 2002). Adaptive optics imaging of TVLM 513-46546 revealed no companions with  $\delta m \lesssim 3$  mag in the range 0.1-15'' (Close et al. 2003).

TVLM 513-46546 was first detected in the radio during a 2 hr observation at 8.5 GHz in Sep. 2001, and exhibited both persistent ( $F_{\nu} \approx 190$   $\mu$ Jy) and flaring emission (Berger 2002), the latter with a peak brightness of 1 mJy, a duration of 15 min, and circular polarization of  $r_c \approx 66\%$ . Subsequent observations from 1.4 to 8.5 GHz in Jan. 2004 revealed a similar level of persistent emission,  $F_{\nu}(1.4) \approx 260$   $\mu$ Jy,  $F_{\nu}(4.9) \approx 280$   $\mu$ Jy, and  $F_{\nu}(8.5) \approx 230$   $\mu$ Jy, with  $r_c \lesssim 15\%$  (Osten et al. 2006b). Observations in Jan. 2005 revealed brighter emission,  $F_{\nu}(4.9) \approx 405$   $\mu$ Jy, and  $F_{\nu}(8.5) \approx 400$   $\mu$ Jy, as well as a claimed periodicity of about 2 hr (Hallinan et al. 2006). Finally, observations in May 2006 uncovered a series of flares with durations of a few minutes,  $\sim 100\%$  circular polarization, and a periodicity of 1.96 hr (Hallinan et al. 2007).

Previous detections of H $\alpha$  emission reveal long term variability, with equivalent widths (EW) ranging from 1.7 to 3.5 Å, or  $L_{\text{H}\alpha}/L_{\text{bol}} \approx 10^{-5}$  (Martin et al. 1994; Reid et al. 2002; Mohanty & Basri 2003).

Our simultaneous observations were obtained on 2007 April 20 UT for a total of 8.8 hr in the radio (04:00-12:48 UT), 8.9 hr in the X-rays (03:47-12:41 UT), and 7 hr in the optical (07:13-14:13 UT). *Swift* UV/optical telescope (UVOT) observations took place intermittently between 03:58 UT and 12:10 UT, with a total on-source exposure time of 8036 s.

### 2.1. Radio

Very Large Array<sup>12</sup> observations were conducted at a frequency of 8.46 GHz in the standard continuum mode with  $2 \times 50$  MHz contiguous bands. Scans of 295 s on source were interleaved with 50 s scans on the phase calibrator J1513+236. The flux density scale was determined using the extragalactic source 3C 48 (J0137+331).

<sup>12</sup>The VLA is operated by the National Radio Astronomy Observatory, a facility of the National Science Foundation operated under cooperative agreement by Associated Universities, Inc.

The data were reduced and analyzed using the Astronomical Image Processing System (AIPS). The visibility data were inspected for quality, and noisy points were removed. To search for source variability, we constructed light curves using the following method. We removed all the bright field sources using the AIPS/IMAGR routine to CLEAN the region around each source, and the AIPS/UVSUB routine to subtract the resulting source models from the visibility data. We then plotted the real part of the complex visibilities at the position of TVLM 513-46546 as a function of time using the AIPS/DFTPL routine. The subtraction of field sources is required since their sidelobes and the change in the shape of the synthesized beam during the observation result in flux variations over the map that may contaminate real variability or generate false variability. The resulting light curves are shown in Figures 1 and 2.

## 2.2. X-Rays

The observations were made with the Chandra/ACIS-S3 (backside-illuminated chip), with TVLM 513-46546 offset from the on-axis focal point by  $15''$ . A total of 29.76 ks were obtained. Data were analyzed using CIAO version 3.3, and counts were extracted in a  $1''$  radius circle centered on the source position. We find a total of 8 counts in the  $0.2 - 2$  keV range, and 2 additional counts with  $kT \approx 10$  keV. Background counts were extracted from annuli centered on the source position, excluding other point sources detected in the observation. We find that 2 background counts are expected within the source extraction aperture, likely corresponding to the two photons with  $kT \approx 10$  keV.

The source counts exhibit a narrow energy range with  $\langle kT \rangle = 930 \pm 250$  eV, corresponding to a typical plasma temperature of  $1.1 \times 10^7$  K. Using this temperature with a Raymond-Smith plasma model we find an energy conversion factor of 1 count =  $3.4 \times 10^{-12}$  erg  $\text{cm}^{-2}$   $\text{s}^{-1}$  ( $0.2 - 2$  keV). Thus, the observed count rate of  $2.69 \times 10^{-4}$   $\text{s}^{-1}$  translates to a flux of  $9.3 \times 10^{-16}$  erg  $\text{cm}^{-2}$   $\text{s}^{-1}$  ( $0.2 - 2$  keV), or a flux density of 1.4 nJy at  $kT = 1$  keV. At the distance of TVLM 513-46546 the corresponding luminosity is  $L_X \approx 1.2 \times 10^{25}$  erg  $\text{s}^{-1}$ , or a ratio of  $L_X/L_{\text{bol}} \approx 10^{-4.9}$ . This detection is at the same level as the quiescent emission from the M8 dwarf VB 10 (Fleming et al. 2003), the faintest X-ray emitting late-M dwarf to date.

We next find that of the 8 detected photons 4 arrive as pairs with separations of 217 and 31 s (Figure 1). The chance probabilities of such short time separations in a 29.76 ks observation are  $1.7 \times 10^{-3}$  and  $3.4 \times 10^{-5}$ , respectively. It is thus possible that the second pair constitutes a flare. If true, the flare luminosity is  $3.1 \times 10^{24}$  erg  $\text{cm}^{-2}$   $\text{s}^{-1}$ , or  $L_X/L_{\text{bol}} \approx 10^{-5.5}$ , the lowest luminosity flare detected from any late-M dwarf to date. The quiescent component would be correspondingly lower,  $L_X/L_{\text{bol}} \approx 10^{-5.0}$ . As we show below, the putative X-ray flare may coincide with the peak of the broadest radio flare.

## 2.3. Optical Spectroscopy

We used<sup>13</sup> the Gemini Multi-Object Spectrograph (GMOS; Hook et al. 2004) mounted on the Gemini-North 8-m telescope with the B600 grating set at a central wavelength of  $5250 \text{ \AA}$ , and with a  $1''$  slit. A series of eighty 300-s exposures were obtained with a readout time of 18 s providing 94% efficiency. The individual exposures were reduced using the `gemini` package in IRAF (for bias subtraction and flat-fielding), and rectification and sky subtraction were performed using the method and software described in Kelson (2003). Wavelength calibration was performed using CuAr arc lamps and air-to-vacuum corrections were applied. The spectrum covers  $3840 - 6680 \text{ \AA}$  at a resolution of about  $5 \text{ \AA}$ .

To measure the equivalent widths of the  $\text{H}\alpha$  and  $\text{H}\beta$  emission lines we use continuum regions centered on  $6551$  and  $6572 \text{ \AA}$ , and on  $4854$  and  $4870 \text{ \AA}$ , respectively. Sample spectra in the low and high Balmer emission state are shown in Figure 3. The  $\text{H}\alpha$  light curve exhibits a clear sinusoidal behavior (Figure 1).

## 2.4. Ultraviolet

The data were obtained with the *Swift*/UVOT in the UVW1 filter ( $\lambda_{\text{eff}} \approx 2510 \text{ \AA}$ ), as a series of 6 images with exposure times ranging from 560 to 1630 s (Figure 1). No source is detected at the position of TVLM 513-46546 in any of the individual exposures, or in the combined image with a total exposure time of 8036 s. We performed photometry on the combined exposure using a circular aperture matched to the PSF of the UVW1 filter ( $2.2''$ ), and found a  $3\sigma$  limit of  $F_\lambda(\text{UVW1}) < 2.4 \times 10^{-18}$  erg  $\text{cm}^{-2}$   $\text{s}^{-1}$   $\text{\AA}^{-1}$ , or a Vega magnitude of  $m(\text{UVW1}) > 23.0$  mag. This limit corresponds to a ratio of UV to bolometric luminosity of  $\lambda L_\lambda/L_{\text{bol}} < 10^{-3.2}$ .

## 3. MULTI-WAVELENGTH EMISSION PROPERTIES

We observed TVLM 513-46546 across a wide wavelength range that traces activity in various layers of the outer atmosphere. The radio emission traces particle acceleration by magnetic processes, and corresponds to gyrosynchrotron radiation or coherent radiation (electron cyclotron maser or plasma emission). The Balmer emission lines are thought to be collisionally excited in the chromosphere, and the X-ray thermal emission arises in the corona.

### 3.1. Quiescent Emission

Using the observed X-ray flux and temperature in the context of bremsstrahlung radiation we can estimate the coronal gas density and pressure. The emissivity is given by:

$$\eta_\nu \approx 7.6 \times 10^{-38} \ln(T/\nu) n_e^2 T^{-1/2} \text{ erg s}^{-1} \text{ cm}^{-3} \text{ Hz}^{-1}, \quad (1)$$

where for TVLM 513-46546,  $T = 1.1 \times 10^7$  and  $\nu = 2.2 \times 10^{17}$  Hz. Assuming a uniform coronal structure extending  $\approx (0.1 - 1)R_*$   $\approx (0.7 - 7) \times 10^9$  cm above the photosphere, we find  $F_{\nu,X} \approx (0.3 - 6) \times 10^{-52} n_e^2$  erg  $\text{s}^{-1}$   $\text{cm}^{-2}$   $\text{Hz}^{-1}$ . From the observed flux density of 1.4 nJy we thus infer an electron density,  $n_e \approx (0.5 - 2) \times 10^{10}$

<sup>13</sup>Observations were obtained as part of program GN-2007A-Q-60.

$\text{cm}^{-3}$ . We note that a coronal structure with a low volume filling factor,  $f$ , would have a correspondingly higher density,  $n_e \propto f^{-1/2}$ . Given this overall uncertainty, the inferred density is similar to what has been found for the M4.5 flare star AD Leo (flares:  $n_e \sim 10^{10} - 10^{11} \text{ cm}^{-3}$ , quiescent:  $n_e < 3 \times 10^{10} \text{ cm}^{-3}$ ; van den Besselaar et al. 2003) and is somewhat lower than in the M3.5 flare star EV Lac ( $n_e \sim 10^{13} \text{ cm}^{-3}$ ; Osten et al. 2006a).

From the temperature and inferred density we find a coronal gas pressure of  $P \approx 10 - 40 \text{ dyne cm}^{-2}$ . This does not take into account turbulent pressure, which at coronal temperatures may in fact be dominant (e.g., Osten et al. 2006a). If the corona is confined by magnetic fields, the required average field strength is thus  $B > \sqrt{8\pi P} \gtrsim 15 - 30 \text{ G}$ .

An alternative estimate of the coronal physical parameters can be provided in the context of the loop model calculated by Rosner et al. (1978). In this model the loop temperature, density, and pressure are related by  $T \approx 1.4 \times 10^3 (P\ell)^{1/3} \text{ K}$ , where it is assumed that the loop apex temperature is similar to the mean coronal temperature. The loop length,  $\ell$ , is determined by the observed X-ray luminosity,  $\ell \approx 2.2 \times 10^{14} f T^{7/2} L_X^{-1} \text{ cm}$ , where  $f$  is the filling factor of the loops. The simple relation between  $T$ ,  $P$ , and  $\ell$  holds as long as  $P \sim \text{const}$  along the loop. This requires the loop length to be less than the pressure scale height,  $H \approx 7.5 \times 10^2 T \text{ cm}$  (for  $R = 0.1 R_\odot$  and  $M = 0.08 M_\odot$ ). From the observed parameters we find  $H \approx 8 \times 10^9 \text{ cm}$  and  $\ell \approx 8 \times 10^{13} f \text{ cm}$ . The condition  $\ell < H$  thus requires a very small filling factor,  $f \lesssim 10^{-4}$ . The pressure inferred from using  $\ell \sim H$  is  $P \approx 60 \text{ dyne cm}^{-2}$ , and the magnetic field required for confinement is thus  $B \gtrsim 40 \text{ G}$ , in good agreement with the value inferred above by assuming a uniform coronal structure.

We now turn to the radio emission. The bremsstrahlung contribution in the radio band is  $F_\nu \approx 0.03 \mu\text{Jy}$ , orders of magnitude lower than even the baseline quiescent emission, which from several flare-free regions of the radio light curve is found to be  $F_\nu(8.5) = 208 \pm 18 \mu\text{Jy}$ . The  $3\sigma$  limit on the fraction of circular polarization of the quiescent component is  $r_c < 25\%$ . Both the flux and degree of circular polarization are similar to those measured in previous observations (§2), indicating that the quiescent component is stable on a multi-year timescale.

Based on the brightness of the radio emission compared to the predicted thermal emission, and its long term stability, we conclude that it is most likely due to gyrosynchrotron radiation. We follow the typical assumption that the mildly relativistic electrons, which produce the radio emission, follow a power law distribution,  $N(\gamma) \propto \gamma^{-p}$  for  $\gamma > \gamma_m$ , with  $p \sim 3$  typical for M and L dwarfs (Gudel et al. 1993b; Berger et al. 2005; Osten et al. 2006b). The gyrosynchrotron emission spectrum is determined by the size of the emission region ( $R$ ), the density of radiating electrons ( $n_e$ ), and the magnetic field strength ( $B$ ) according to (Dulk & Marsh 1982):

$$r_c = 0.3 \times 10^{1.93\cos\theta - 1.16\cos^2\theta} (3 \times 10^3 / B)^{-0.21 - 0.37\sin\theta}, \quad (2)$$

$$\nu_m = 1.8 \times 10^4 (\sin\theta)^{0.5} (n_e R)^{0.23} B^{0.77} \text{ Hz}, \quad (3)$$

$$F_{\nu,m} = 2.5 \times 10^{-41} B^{2.48} R^3 n_e (\sin\theta)^{-1.52} \mu\text{Jy}, \quad (4)$$

where  $\theta$  is the angle between the magnetic field and the line of sight.

From previous observations of TVLM 513-46546 it appears that the peak of the quiescent emission spectrum is  $\nu_m \approx 5 \text{ GHz}$  (Osten et al. 2006b). Using the limit  $r_c < 25\%$ , we infer a magnetic field strength,  $B \lesssim 10 - 740 \text{ G}$ , for  $\theta = 20 - 80^\circ$ . With this range we find  $R \sim (0.8 - 8) \times 10^{10} \text{ cm}$ , and  $n_e \sim 100 - 1.3 \times 10^{10} \text{ cm}^{-3}$ ; the latter range is for  $\theta = 80^\circ$  to  $20^\circ$ . A comparison to the coronal density estimated from X-rays indicates  $\theta \sim 20 - 30^\circ$ , and hence  $R \sim \text{few} \times 10^{10} \text{ cm}$  and  $B \lesssim \text{few} \times 10^2 \text{ G}$ . The inferred field strength is consistent with the value required for confinement of the X-ray emitting coronal plasma as derived above.

Finally, we turn to the observed  $\text{H}\alpha$  emission. The light curve exhibits clear sinusoidal behavior with a range of equivalent widths of  $1.5 - 5.5 \text{ \AA}$  (Figure 1). The sinusoidal behavior indicates that the line is likely modulated by the rotation of TVLM 513-46546 rather than flares, and the emission is thus persistent in origin, at least on the timescale of our observation. Walkowicz et al. (2004) determined a multiplicative factor,  $\chi \equiv f_{\lambda 6560} / f_{\text{bol}}$ , to convert  $\text{H}\alpha$  EW to  $L_{\text{H}\alpha} / L_{\text{bol}}$ . For TVLM 513-46546, the observed  $I - K = 4.3 \text{ mag}$  indicates  $\log \chi \approx -5.3$ , which matches the average value for spectral type M8.5 (Walkowicz et al. 2004). Thus, for the full range of EWs we find  $\log(L_{\text{H}\alpha} / L_{\text{bol}}) \approx -4.6$  to  $-5.1$ . This covers the typical range of  $\text{H}\alpha$  emission observed from M8.5 dwarfs (West et al. 2004), as well as the range of EWs from past observations of this source (§2). We return to the implications of the sinusoidal variations in §3.3.

Since the X-ray and  $\text{H}\alpha$  emission appear to be persistent, we can gain insight into the physical processes in the outer atmosphere by examining the energy scale in each band. In early dMe stars there is evidence that the quiescent chromosphere is heated by downward directed coronal X-ray emission (Cram 1982). Nearly half of the absorbed energy will be radiatively lost in the Balmer lines, primarily  $\text{H}\alpha$  (Cram 1982). Here we find that the ratio  $L_{\text{H}\alpha} / L_X \approx 2$  is in rough agreement with this overall model, taking into account the overall uncertainties in the X-ray and  $\text{H}\alpha$  luminosities. However, as noted by Cram (1982), any significant asymmetry in the coronal structure (e.g., extended loops) will substantially reduce the X-ray flux directed at the chromosphere. Since we find that the  $\text{H}\alpha$  line by itself already accounts for the maximal coronal heating rate, this model of chromospheric heating requires a uniform coronal structure.

Alternatively, the marginal excess chromospheric luminosity may indicate that the structure of the outer atmosphere in this late-M dwarf is markedly different than in early dMe stars. Potentially, the  $\text{H}\alpha$  emission is dominated by a non-chromospheric component. As we discuss below, in the context of the periodic emission, it is possible that the  $\text{H}\alpha$  emission region is a more extended ‘‘bubble’’ that co-rotates with the star.

### 3.2. Radio Flares

In addition to the persistent emission in the radio band we detect several distinct short duration ( $\delta t \sim 2 - 15 \text{ min}$ )

flares, and a single broad brightening with a duration of about 1 hr (Figures 1 and 2). These flares range in peak flux density from 2 to 5.5 mJy. Our observations allow the detection of flares to a  $5\sigma$  sensitivity of about 3.5 mJy in a single 5 s integration. In Figure 2 we provide a zoom-in on the most distinct flares, including both the total intensity light curve and the circular polarization light curve. About half of the flares exhibit left circular polarization, while the other half exhibit right circular polarization, with overall fractions of  $\sim 50 - 100\%$ . There is no apparent regularity in the duration, brightness, arrival time, or circular polarization of the flares.

The apparently random sense of circular polarization (right- vs. left-handed) and flare arrival times suggest that the flares are produced in unrelated regions. This is contrary to the model proposed by Hallinan et al. (2007) to explain their detection of periodic flares, with  $P = 1.96$  hr well-matched to the rotation of TVLM 513-46546. These authors point to emission from a distinct region that is stable over at least several rotation periods. The absence of a similar behavior in our data suggests that this stability is limited to  $\lesssim 1$  yr.

The variation in the sense of circular polarization from one flare to the next is also different from the uniform sense of polarization observed in radio flares from UV Cet (M5.5) and YZ CMi (M4.5). Flares in these two stars show consistent right-handed and left-handed polarization, respectively, which has been interpreted as a signature particle acceleration in a toroidal dipole field (Kellett et al. 2002). The behavior of radio flares from TVLM 513-46546 in the current observation thus points to a multi-polar field configuration.

While the quiescent radio emission is due to gyrosynchrotron radiation, the short durations and large fraction of circular polarization of the flares point to emission by coherent processes. The electron cyclotron maser (ECM) process leads to emission at the fundamental cyclotron frequency,  $\nu_c = 2.8 \times 10^6 B$  Hz, while plasma radiation is dominated by the fundamental plasma frequency,  $\nu_p = 9 \times 10^3 n_e^{1/2}$  Hz. In the ECM case the magnetic field strength inferred from the detection of flares at 8.46 GHz is  $B \approx 3$  kG, while in the case of plasma radiation we infer an electron density of  $n_e \approx 9 \times 10^{11} \text{ cm}^{-3}$ . The latter should be used as an upper limit in the ECM model.

In the standard picture of the electron cyclotron maser (e.g., Melrose & Dulk 1982), electrons with a large pitch angle are reflected at the legs of the magnetic loop, while those with smaller angles precipitate into and heat the chromosphere. This process repeats, with the rise time of the emitted flare presumably reflecting the particle acceleration timescale. The flare decay reflects the time to precipitate out of the magnetic trap, and is thus related to the loss rate,  $\tau \sim [(\Omega_L/4\pi)v/\ell]^{-1}$ , where  $\Omega_L$  is the solid angle of the loss cones,  $v$  is the electron velocity, and  $\ell$  is the transit length (Melrose & Dulk 1982). From our observations at 8.5 GHz we infer  $v \sim c$ , and hence  $\tau \sim 30$  s leads to,  $\ell \sim 10^{12} (\Omega_L/4\pi)$  cm. The actual size of the loop region is likely to be much smaller since the accelerated electrons traverse the field lines multiple times before the maser process ceases. Thus, whereas in the case of the

periodic outbursts a stable, dipolar field configuration was inferred (Hallinan et al. 2007), here it is likely that the emission is arising from a tangled, multi-polar field.

Finally, the ECM processes is supposed to provide coronal and chromospheric heating as electrons precipitate out of the trap, and thus lead to increased H $\alpha$  and X-ray emission. From Figure 1 it is clear that this is not the case for TVLM 513-46546. None of the flares radio are accompanied by an increase in either the H $\alpha$  or X-ray emission. This may provide further support to the proposed tangled field configuration, since it will lead to chromospheric and coronal effects on a small scale that may go undetected when averaged over the stellar disk.

### 3.3. Sinusoidal H $\alpha$ Emission

As noted above the H $\alpha$  and H $\beta$  emission lines exhibit sinusoidal variations with a periodicity of about 2 hours (Figure 1). This indicates that the likely origin of the Balmer line modulation is the rotation of TVLM 513-46546. Indeed with  $R_* \approx 7 \times 10^9$  cm, the 2-hour period requires a rotation velocity of  $v \approx 60 \text{ km s}^{-1}$ , in perfect agreement with the observed  $v \sin i \approx 60 \text{ km s}^{-1}$ . If the Balmer lines are modulated by rotation, this indicates an inclination of the rotation axis relative to the line of sight of  $i \approx 90^\circ$ .

The likely connection to stellar rotation points to a large scale ( $f \sim 50\%$ ) hot spot located on one hemisphere of TVLM 513-46546, or an emission ‘‘bubble’’ that may extend to several times the stellar radius, and is occulted by the star for about half a rotation period. As noted above, the latter scenario may be relevant since the observed H $\alpha$  luminosity appears to exceed the X-ray luminosity by a factor of a few, raising the possibility of an H $\alpha$  emission region distinct from the chromosphere. The fact that the Balmer lines do not completely disappear during the light curve minima suggests that in both scenarios the solid angle subtended by the emission region is larger than the stellar disk, or alternatively, that the minima represent the baseline chromospheric emission, while the rotation of an extended bubble or a hot spot into our line of sight produces the maxima.

It also appears from the H $\alpha$  light curve that the peak equivalent width decreases with time (Figure 1). The first peak has EW  $\approx 5.5 \text{ \AA}$  followed by about  $4.5 \text{ \AA}$  for the two subsequent peaks, and about  $3.8 \text{ \AA}$  for the fourth peak. While our observations start during the decline of a preceding cycle, an extrapolation back to the time of the expected peak indicates an equivalent width of at least  $6 \text{ \AA}$ . The equivalent widths at the minima, however, appear to be more stable, with perhaps a slight decrease from 2 to  $1.5 \text{ \AA}$  during our observation. These trends suggest that the hot spot or extended bubble may be transitory, possibly excited by an energetic event prior to the beginning of our observations. Extrapolating the observed trend, we find that the peak H $\alpha$  equivalent width will match the baseline level of  $1.5 \text{ \AA}$  about 7 hrs after the end of our observation. Future observations of TVLM 513-46546 are crucial for assessing whether this is in fact a transient feature.

We further find no clear correspondence between the peaks of H $\alpha$  emission and the radio flares. In fact, the opposite may be the case. The three H $\alpha$  minima that

have simultaneous radio coverage appear to roughly coincide with radio flares. If we extrapolate the H $\alpha$  light curve back in time, we find that a previous minimum also appears to coincide with a radio flare (at about 05:40 UT). However, other radio flares, including the brightest one detected, do not coincide with observed or extrapolated H $\alpha$  minima, suggesting that this anti-correlation between H $\alpha$  and radio emission may be a result of small number statistics.

The detection of a 2 hour period in two different emission bands and at two different times with no clear correspondence indicates that the radio flares are not sufficiently energetic, or impact a large enough scale to influence the chromosphere. This behavior also suggests that the magnetic field configuration of TVLM 513-46546 may be composed of a large-scale dipolar field, as well as a more compact and tangled component, which give rise to periodic signals at different times and wavebands.

#### 4. LACK OF RADIO/X-RAY CORRELATION

TVLM 513-46546 is only the third ultracool dwarf to be observed simultaneously in the radio and X-rays, allowing a continued investigation of the radio/X-ray correlation in these objects. Coronally active stars up to spectral type M7, including the Sun, exhibit a tight correlation between their radio and X-ray emission (Guedel & Benz 1993; Benz & Guedel 1994). The persistent emission follows a linear trend,  $L_R \approx 3 \times 10^{-16} L_X \text{ Hz}^{-1}$ , which extends over 6 orders of magnitude in  $L_R$  (Guedel & Benz 1993), while for flares the relation is  $L_R \approx 5.4 \times 10^{-27} L_X^{1.37} \text{ Hz}^{-1}$  over 8 orders of magnitude in  $L_R$  (Benz & Guedel 1994); see Figure 4.

From several previous (non-simultaneous) observations it has become clear that the above correlations break down in at least some ultracool dwarfs (Berger et al. 2001; Berger 2002; Berger et al. 2005; Berger 2006), with a clear transition occurring at spectral type M7 (Berger 2006). This conclusion was supported by our simultaneous observations of the L3.5 dwarf 2MASS J00361617+1821104 (Berger et al. 2005). Here we find continued evidence for this trend. Using the persistent radio and X-ray luminosities we find  $L_R/L_X \approx 2.3 \times 10^{-12} \text{ Hz}^{-1}$ , a factor of about 7800 times larger than expected. This is similar to the level of excess radio emission observed in the previous late-M and L dwarfs. If we take into account the flaring emission, with a typical peak luminosity of  $L_R \approx 4 \times 10^{14} \text{ erg cm}^{-2} \text{ s}^{-1} \text{ Hz}^{-1}$ , and assume that the single X-ray photon pair with  $L_X \approx 3 \times 10^{24} \text{ erg cm}^{-2} \text{ s}^{-1}$  is indeed a flare (§2.2), we find that for flares  $L_R/L_X \approx 1.3 \times 10^{-10} \text{ Hz}^{-1}$ , a factor of about  $10^7$  larger than expected.

The radio/X-ray correlation has been interpreted in the context of the Neupert effect (Neupert 1968). In this scenario, the radio emission is produced when coronal magnetic loops reconnect and create a current sheet along which ambient electrons are accelerated. The accelerated electrons in turn drive an outflow of hot plasma into the corona as they interact with and evaporate the underlying chromospheric material. The interaction of the outflowing plasma with the electrons produces X-ray emission via the bremsstrahlung process. This mechanism points to a causal connection between particle acceleration, which is

the source of radio emission, and plasma heating, which results in X-ray emission. Thus, the X-ray thermal energy should simply be related by a constant of proportionality to the integrated radio flux. The breakdown in the radio/X-ray correlation, and the clear lack of correspondence between the radio flares observed on TVLM 513-46546 and its X-ray emission suggest that the heating of coronal material is generally inefficient in objects later than M7. This may be due to the short lifetime and small size of the flare emitting regions (i.e., in the case that they arise from highly tangled and multi-polar fields), or to lower efficiency of coronal heating so that the bulk of the coronal emission is at temperatures lower than  $kT \sim 1 \text{ keV}$ .

#### 5. DISCUSSION AND CONCLUSIONS

We presented simultaneous radio, X-ray, UV, and optical spectroscopic observations of the M8.5 dwarf TVLM 513-46546 that probe magnetic activity and its influence on the stellar chromosphere and corona. These observations are the first in a series of several objects that span the sparsely-studied spectral type range M7–L3, over which the magnetic activity appears to exhibit a change in behavior compared to early spectral types. We find that TVLM 513-46546 exhibits a wide range of both quiescent and flaring activity that includes radio emission from large and small scale regions, coronal soft X-ray emission, and sinusoidal and periodic Balmer line emission from a chromospheric hot spot or an extended structure with a covering fraction of about 50%.

Quantitatively, we find that the quiescent radio emission is produced on the scale of the entire stellar disk, with a magnetic field of  $\sim 10^2 \text{ G}$ . From portions of the light curve that are free of flares we see no evidence for variability of this persistent component. Moreover, the similarity in flux level to observations carried over the past 6 years indicates that the magnetic field is stable on timescales significantly longer than the convective turnover time,  $\tau_{\text{conv}} \sim 10^2 \text{ d}$  (Chabrier & Baraffe 2000). This is similar to the situation we observed in 2MASS J00361617+1821104 (L3.5), with a periodic radio signal that was stable over at least 3 years (Berger et al. 2005).

We also find from a comparison of the radio and X-ray data that the magnetic field axis is likely highly inclined relative to the rotation axis of TVLM 513-46546, which is inferred from the 2-hour period of the H $\alpha$  emission to be about  $90^\circ$  (§3.3). This is an interesting result in the context of magnetic dynamo models of fully convective stars. Chabrier & Küker (2006) and Dobler et al. (2006) found that the  $\alpha^2$  dynamo, which relies on a stratified and rotating turbulent medium, leads to a non-axisymmetric field with an overall configuration that lies in the equatorial plane. This seems to be supported by our observations.

The X-ray emission requires a corona with  $T \approx 10^7 \text{ K}$  and a density of  $n_e \sim 10^{10} \text{ cm}^{-3}$ , similar to those of early M dwarfs. The inferred coronal gas pressure requires a magnetic field strength of at least  $\sim 10 - 40 \text{ G}$  for confinement, in good agreement with the radio-derived field strength. The energy input from the X-ray emitting corona is similar to, or somewhat smaller than, the radiative losses in the Balmer emission lines, indicating that

the chromosphere is at least partly heated by the overlying corona. It is possible, however, that the somewhat elevated chromospheric luminosity is the result of an energy input process that took place before the start of our observations. This latter possibility is supported by the apparently decreasing level of peak  $H\alpha$  flux during our observation, and the nearly constant baseline level traced by the light curve minima. Indeed, the  $H\alpha$  luminosity during the minima is about half of the X-ray luminosity.

In addition to the persistent emission, we detect a large number of radio flares with a range of peak fluxes, durations, and degrees of circular polarization. The overall short durations of the flares and large degree of circular polarization are indicative of coherent emission. In the context of the electron cyclotron maser mechanism, the inferred magnetic field is about 3 kG, similar to fields on the most active early M dwarfs (Saar & Linsky 1985; Johns-Krull & Valenti 1996). Similar flares have been detected in previous observations of TVLM 513-46546, but with a 2 hour periodicity that is absent in our data. The 2 hour period was attributed to compact polar regions in a dipolar field rotating in and out of our line of sight (Hallinan et al. 2007). The durations of the flares detected here, and their random arrival times and sense of circular polarization, point instead to a tangled and multi-polar field. Thus, the conditions required for coronal coherent radio flares exist on long timescales, but the change in behavior may signal a shift in the field configuration on  $\lesssim 1$  yr timescales. The inferred multi-polar nature of the field is again in good agreement with models of the  $\alpha^2$  dynamo, which suggest that the bulk of the energy is in the quadrupolar and higher order components.

Unlike in the radio flares, we do find clear  $H\alpha$  periodicity ( $P \approx 2$  hr), with a sinusoidal light curve that reveals the presence of a chromospheric hot spot, or an extended bubble, with a covering fraction of about 50%. It is unclear whether this emission region is stable over timescales longer than about 1 day, but the decrease in peak flux between subsequent rotations may point to a transient nature that may be similar to the one now inferred in the radio band. The observed 2-hour period is well matched to the measured rotation velocity of TVLM 513-46546, and indicates a rotation axis inclination of about 90 deg. The existence of such an extended structure provides additional support for a large-scale field that dominates the quiescent radio and X-ray emission.

The general wisdom in the study of magnetic activity and its impact on the outer atmosphere is that the input of magnetic energy results in a series of related events that heat the corona and chromosphere and result in correlated X-ray, radio, and optical line emission. This idea is supported by observations of the Sun, as well as various samples of early M dwarfs. The observations presented here show no clear evidence for any correlation between the various activity bands. In particular, the quiescent radio emission is over-luminous by nearly 4 orders of magnitude compared to predictions from the radio/X-ray correlation. Similarly, the radio flares do not appear to correlate with the  $H\alpha$  variability. Finally, it is possible that the X-ray flux incident on the chromosphere is not sufficient

to produce the observed  $H\alpha$  luminosity (particularly if we include the contribution from higher order Balmer lines).

Taking these various observations and inferences into account we therefore conclude that the observations of TVLM 513-46546 indicate that:

- Ultracool dwarfs exhibit clear evidence for intense magnetic activity that is not diminished compared to early M dwarfs. This activity is manifested most clearly in the centimeter radio band, but also in X-rays and Balmer line emission.
- Both a chromosphere and a corona appear to exist, with luminosities relative to the bolometric luminosity that are in line with other objects of similar spectral type, and are significantly lower (by  $\sim 2$  orders of magnitude) compared to early M dwarfs.
- The dissipation of magnetic energy leads to intense radio emission, but it does not have a clear effect on chromospheric and coronal emission, both temporally and in terms of overall luminosity. The radio/X-ray correlation is violated by about 4 orders of magnitude.
- The decoupling of magnetic dissipation (as evidenced by radio emission) from chromospheric and coronal emission may be due to changes in the structure and scale of the magnetic field or the outer atmosphere. This is possibly supported by the higher chromospheric luminosity compared to the coronal luminosity.
- The presence of a steady large-scale magnetic field, as well as a multi-polar component, support current models of  $\alpha^2$  dynamos in fully convective stars.

Simultaneous multi-wavelength observations of several additional ultracool dwarfs are in progress. We expect that with this larger sample, and with the longer time baselines of our observations compared to typical studies, we can begin to address in detail the range of quiescent and variable activity, and the absence or presence of the correlations that appear to exist in the early M dwarfs. Ultimately, these observations should reveal the energy and size scale of the magnetic field, and thus provide a detailed view of the magnetic generation process in fully convective stars.

We thank the Chandra, Gemini, VLA, and Swift schedulers for their invaluable help in coordinating these observations. This work has made use of the SIMBAD database, operated at CDS, Strasbourg, France. Based in part on observations obtained at the Gemini Observatory, which is operated by the Association of Universities for Research in Astronomy, Inc., under a cooperative agreement with the NSF on behalf of the Gemini partnership: the National Science Foundation (United States), the Science and Technology Facilities Council (United Kingdom), the National Research Council (Canada), CONICYT (Chile), the Australian Research Council (Australia), CNPq (Brazil) and CONICET (Argentina). Data from the UVOT instrument on Swift were used in this work. Swift is an international observatory developed and operated in the US, UK and

Italy, and managed by NASA Goddard Space Flight Center with operations center at Penn State University. Support for this work was provided by the National Aeronautics and Space Administration through Chandra Award Number G07-8014A issued by the Chandra X-ray Observatory Center, which is operated by the Smithsonian As-

trophysical Observatory for and on behalf of the National Aeronautics Space Administration under contract NAS8-03060. E.B. is supported by NASA through Hubble Fellowship grant HST-01171.01 awarded by the STScI, which is operated by AURA, Inc., for NASA under contract NAS 5-26555.

#### References

- Antonova, A., Doyle, J. G., Hallinan, G., Golden, A., & Koen, C. 2007, ArXiv e-prints, 707
- Audard, M., Osten, R. A., Brown, A., Briggs, K. R., Guedel, M., Hodges-Kluck, E., & Gizis, J. E. 2007, ArXiv e-prints, 707
- Basri, G., & Marcy, G. W. 1995, *AJ*, 109, 762
- Benz, A. O., & Guedel, M., 285, 621
- Berger, E. 2002, *ApJ*, 572, 503
- Berger, E. 2006, *ApJ*, 648, 629
- Berger, E., et al. 2001, *Nature*, 410, 338
- Berger, E., et al. 2005, *ApJ*, 627, 960
- Burgasser, A. J., & Putman, M. E. 2005, *ApJ*, 626, 486
- Chabrier, G., & Baraffe, I. 2000, *ARA&A*, 38, 337
- Chabrier, G., & Küker, M. 2006, *A&A*, 446, 1027
- Close, L. M., Siegler, N., Freed, M., & Biller, B. 2003, *ApJ*, 587, 407
- Cram, L. E. 1982, *ApJ*, 253, 768
- Dahn, C. C., et al. 2002, *AJ*, 124, 1170
- Dobler, W., Stix, M., & Brandenburg, A. 2006, *ApJ*, 638, 336
- Dulk, G. A., & Marsh, K. A. 1982, *ApJ*, 259, 350
- Fleming, T. A., Giampapa, M. S., & Garza, D. 2003, *ApJ*, 594, 982
- Fleming, T. A., Giampapa, M. S., Schmitt, J. H. M. M., & Bookbinder, J. A. 1993, *ApJ*, 410, 387
- Gizis, J. E., Monet, D. G., Reid, I. N., Kirkpatrick, J. D., Liebert, J., & Williams, R. J. 2000, *AJ*, 120, 1085
- Güdel, M. 2002, *ARA&A*, 40, 217
- Gudel, M., Schmitt, J. H. M. M., Bookbinder, J. A., & Fleming, T. A. 1993a, *ApJ*, 415, 236
- Gudel, M., Schmitt, J. H. M. M., Bookbinder, J. A., & Fleming, T. A. 1993b, *ApJ*, 415, 236
- Guedel, M., & Benz, A. O. 1993, *ApJ*, 405, L63
- Guedel, M., Benz, A. O., Schmitt, J. H. M. M., & Skinner, S. L. 1996, *ApJ*, 471, 1002
- Hallinan, G., Antonova, A., Doyle, J. G., Bourke, S., Brisken, W. F., & Golden, A. 2006, *ApJ*, 653, 690
- Hallinan, G., et al. 2007, *ApJ*, 663, L25
- Hawley, S. L., et al. 1995, *ApJ*, 453, 464
- Hook, I. M., Jørgensen, I., Allington-Smith, J. R., Davies, R. L., Metcalfe, N., Murowinski, R. G., & Crampton, D. 2004, *PASP*, 116, 425
- Johns-Krull, C. M., & Valenti, J. A. 1996, *ApJ*, 459, L95
- Kellett, B. J., Bingham, R., Cairns, R. A., & Tsikoudi, V. 2002, *MNRAS*, 329, 102



- Kelson, D. D. 2003, *PASP*, 115, 688
- Liebert, J., Kirkpatrick, J. D., Cruz, K. L., Reid, I. N., Burgasser, A., Tinney, C. G., & Gizis, J. E. 2003, *AJ*, 125, 343
- Martin, E. L., Rebolo, R., & Magazzu, A. 1994, *ApJ*, 436, 262
- Melrose, D. B., & Dulk, G. A. 1982, *ApJ*, 259, 844
- Mohanty, S., & Basri, G. 2003, *ApJ*, 583, 451
- Mohanty, S., Basri, G., Shu, F., Allard, F., & Chabrier, G. 2002, *ApJ*, 571, 469
- Neupert, W. M. 1968, *ApJ*, 153, L59
- Osten, R. A., Hawley, S. L., Allred, J., Johns-Krull, C. M., Brown, A., & Harper, G. M. 2006a, *ApJ*, 647, 1349
- Osten, R. A., Hawley, S. L., Bastian, T. S., & Reid, I. N. 2006b, *ApJ*, 637, 518
- Pallavicini, R., Golub, L., Rosner, R., Vaiana, G. S., Ayres, T., & Linsky, J. L. 1981, *ApJ*, 248, 279
- Phan-Bao, N., Osten, R. A., Lim, J., Martín, E. L., & Ho, P. T. P. 2007, *ApJ*, 658, 553
- Pizzolato, N., Maggio, A., Micela, G., Sciortino, S., & Ventura, P. 2003, *A&A*, 397, 147
- Reid, I. N., Kirkpatrick, J. D., Gizis, J. E., & Liebert, J. 1999, *ApJ*, 527, L105
- Reid, I. N., Kirkpatrick, J. D., Liebert, J., Gizis, J. E., Dahn, C. C., & Monet, D. G. 2002, *AJ*, 124, 519
- Rosner, R., Golub, L., & Vaiana, G. S. 1985, *ARA&A*, 23, 413
- Rosner, R., Tucker, W. H., & Vaiana, G. S. 1978, *ApJ*, 220, 643
- Rutledge, R. E., Basri, G., Martín, E. L., & Bildsten, L. 2000, *ApJ*, 538, L141
- Saar, S. H., & Linsky, J. L. 1985, *ApJ*, 299, L47
- van den Besselaar, E. J. M., Raassen, A. J. J., Mewe, R., van der Meer, R. L. J., Güdel, M., & Audard, M. 2003, *A&A*, 411, 587
- Vilhu, O., & Walter, F. M. 1987, *ApJ*, 321, 958
- Walkowicz, L. M., Hawley, S. L., & West, A. A. 2004, *PASP*, 116, 1105
- West, A. A., et al. 2004, *AJ*, 128, 426

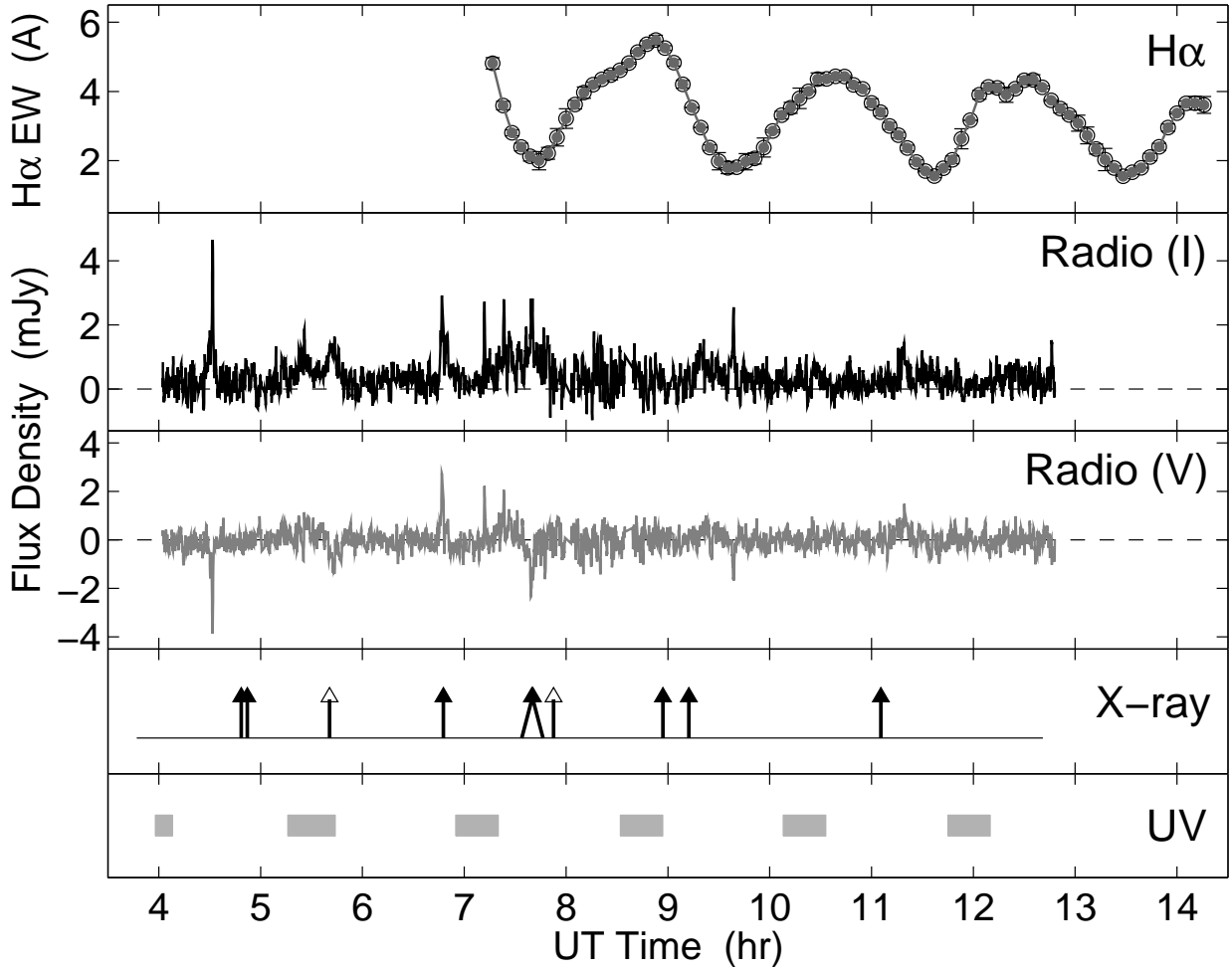


FIG. 1.— Radio,  $H\alpha$ , UV, and X-ray of TVLM 513-46546. The arrival times of the X-ray photons are shown with arrows. Empty arrows correspond to likely background events with  $kT \gtrsim 10$  keV; two are expected from the background count rate. Times of UV coverage are marked by gray squares; no UV emission is detected. The  $H\alpha$  emission is clearly sinusoidal and periodic, with  $P \approx 2$  hr matching the rotation period of TVLM 513-46546, with an implied  $\sin i \approx 1$ . There is no clear correspondence between the various emission bands, with the possible exception of an X-ray photon pair that coincides with the broadest radio flare (at about 07:40 UT).

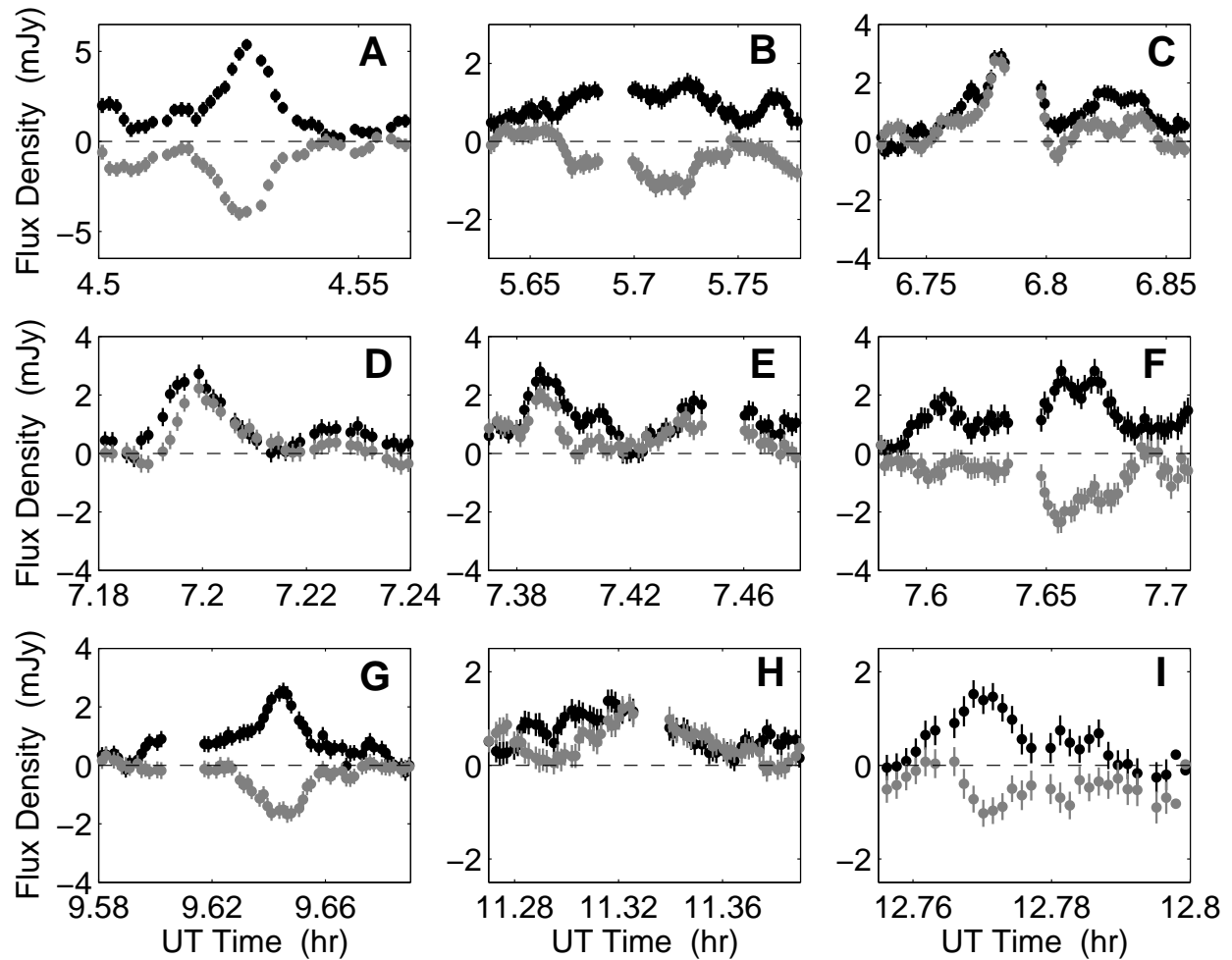


FIG. 2.— Zoom-in on individual radio flares. Total intensity (black) and circularly polarized flux (gray) are shown. The flares exhibit diverse behavior in terms of duration, amplitude, and fraction and sense of circular polarization.

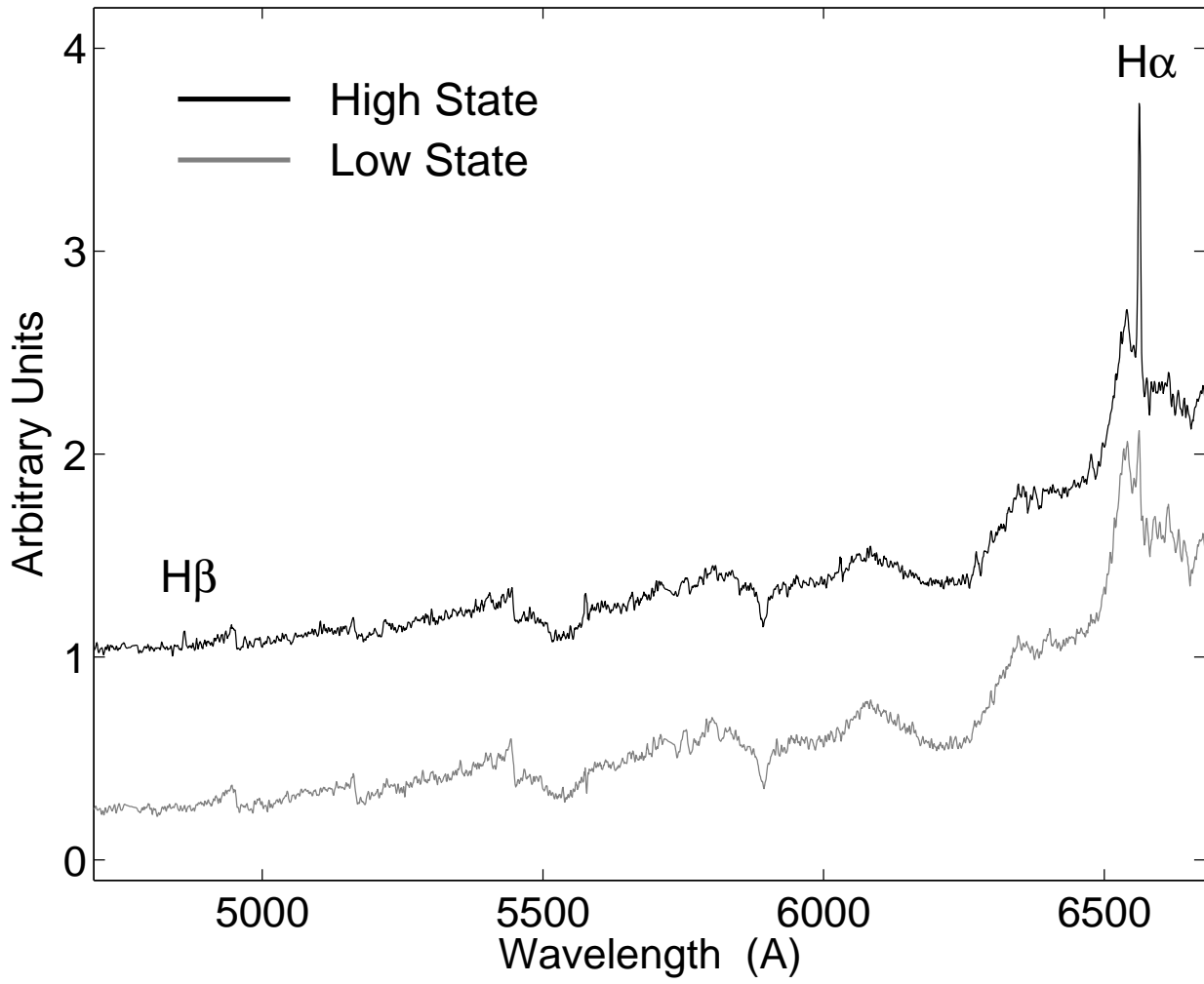


FIG. 3.— Sample optical spectra of TVLM 513-46546 in the high and low Balmer emission line states. The high state spectrum has been offset upward for clarity.

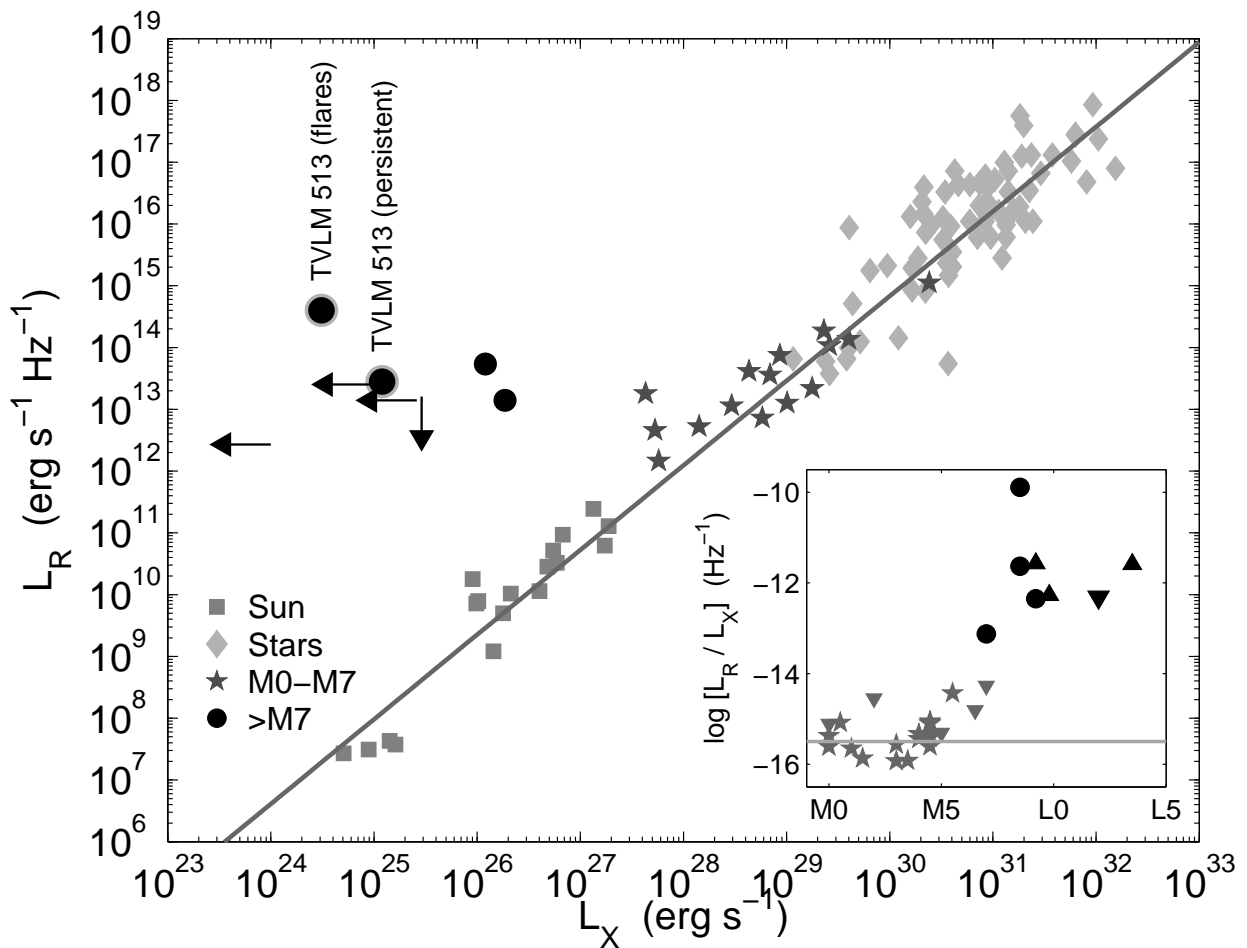


FIG. 4.— Radio vs. X-ray luminosity for stars exhibiting coronal activity. Data for late-M and L dwarfs are from Rutledge et al. (2000), Berger et al. (2001), Berger (2002), Berger et al. (2005), Burgasser & Putman (2005), Berger (2006), and Audard et al. (2007), while other data are taken from Güdel (2002) and references therein. Data for the Sun include impulsive and gradual flares, as well as microflares. The strong correlation between  $L_R$  and  $L_X$  is evident, but it begins to break down around spectral type M7 (see inset).